

Observation of quasiparticles with one-fifth of an electron's charge

M. Reznikov*†, R. de Picciotto*†, T. G. Griffiths*, M. Heiblum* & V. Umansky*

* Braun Center for Submicron Research, Department of Condensed Matter Physics, Weizmann Institute of Science, Rehovot 76100, Israel

The fractional quantum Hall effect¹ occurs in the conduction properties of a two-dimensional electron gas subjected to a strong perpendicular magnetic field. In this regime, the Hall conductance shows plateaux, or fractional states, at rational fractional multiples of e^2/h , where e is the charge of an electron and h is Planck's constant. The explanation¹⁻³ of this behaviour invokes strong Coulomb interactions among the electrons that give rise to fractionally charged quasiparticles which can be regarded as non-interacting current carriers¹⁻⁵. Previous studies^{4,5} have demonstrated the existence of quasiparticles with one-third of an electron's charge, the same fraction as that of the respective fractional state. An outstanding ambiguity is therefore whether these studies measured the charge or the conductance. Here we report the observation of quasiparticles with a charge of $e/5$ in the $2/5$ fractional state, from measurements of shot noise in a two-dimensional electron gas⁴. Our results imply that charge can be measured independently of conductance in the fractional quantum Hall regime, generalizing previous observations of fractionally charged quasiparticles.

In the fractional quantum Hall (FQH) regime, the first Landau level is partly populated, or 'fractionally filled'. Laughlin's explanation of the FQH effect¹⁻³ involved the emergence of new, fractionally charged, quasiparticles. Shot-noise measurements^{4,5} have confirmed the existence of these quasiparticles in the FQH regime. Shot noise, resulting from the granular nature of the particles, is proportional to the charge of the current carriers, in this case quasiparticles^{4,5}. In these experiments a quantum point contact (QPC) embedded in a two-dimensional electron gas (2DEG), serving as a potential constriction, was used as an electronic 'beam splitter'. Its purpose is to partly reflect back the incoming current and lead to partitioning of carriers and hence to shot noise. An applied magnetic field corresponding to fractional filling factors (in the bulk far from the QPC) of $\nu_B = 1/3$ in ref. 4 or $2/3$ in ref. 5, was employed. Charge was deduced via the generalized equation for shot noise of non-interacting particles (the classical and simplified version is the Schottky formula: $S = 2qI_B$, with S the low-frequency spectral density of current fluctuations, I_B the reflected current, and q the charge of the current-carrying particle). For small reflection by the QPC (small I_B) the quasiparticle's charge was found to be $e/3$ (ref. 4 and 5), as predicted theoretically⁶⁻⁸. The theories are based on the chiral Luttinger-liquid model and are applicable only for Laughlin fractional states, for example, $1/3$, $1/5$, and so on. For other, more general filling factors (such as $\nu = 2/5$), however, such calculations become exceedingly complicated. Still, one can gain insight into the characteristics of the expected shot noise in such cases by considering the more intuitive composite fermion (CF) model^{9,10}.

Laughlin suggested that in the FQH regime the current is carried by weakly interacting quasiparticles with charge $q = e/(2pn + 1)$, where e is the electronic charge. The fractional filling factor $\nu = p/(2pn + 1)$ determines the conductance of the sample $g = \nu g_0$, with $g_0 = e^2/h$ being the quantum conductance. Within

the CF model, fractional filling factors for electrons of the form $\nu = p/(2pn + 1)$ are identified as integer filling factors of CFs, $\nu_{CF} = p$. Each CF is composed of a single electron with $2n$ quanta of magnetic flux (derived from the applied magnetic field) attached to it (each flux quantum is $\phi_0 = h/e$). Here we deal with the simplest family of CFs, with only two flux quanta attached to each electron ($n = 1$). A filling factor $\nu = 1/3$ then corresponds to the simplest fraction $p = 1$ while $\nu = 2/5$ corresponds to $p = 2$, that is, two CF Landau levels are filled. The effective magnetic field sensed by the CFs is $B - 2n_s(h/e)$, with n_s the density of the 2DEG and B the magnetic field. Under this, weaker, effective magnetic field the CFs are usually considered as non-interacting quasiparticles (though a justification of this assertion is not solid). Shot noise, induced by the QPC, is thus recognized as partition noise—associated with partial reflection of CFs in integer Landau levels (referred to below as 'CF channels'). This scheme is similar to that taking place at a QPC reflector at zero applied magnetic field¹¹⁻¹⁴. The shot noise in a weakly reflected channel p (filling factor $p/(2p + 1)$) is expected¹⁵ to correspond to quasiparticles with charge $q = e/(2p + 1)$.

It is important to examine the noise properties at fractional filling factors in which the value of the charge in units of e is expected to differ from the filling factor. Observation of a charge $e/(2p + 1)$ for $p > 1$ would prove that our charge measurement is not simply a different way to measure the conductance (or the filling factor)¹⁶. An obvious experimental target is the filling factor $\nu = 2/5$, where the charge of the current-carrying quasiparticles is expected to be $(1/5)e$ while the conductance is $(2/5)g_0$.

The contribution of each one-dimensional channel without magnetic field is known to be equal to the quantum conductance $g_0 = e^2/h$. However, the conductance of each CF channel has a

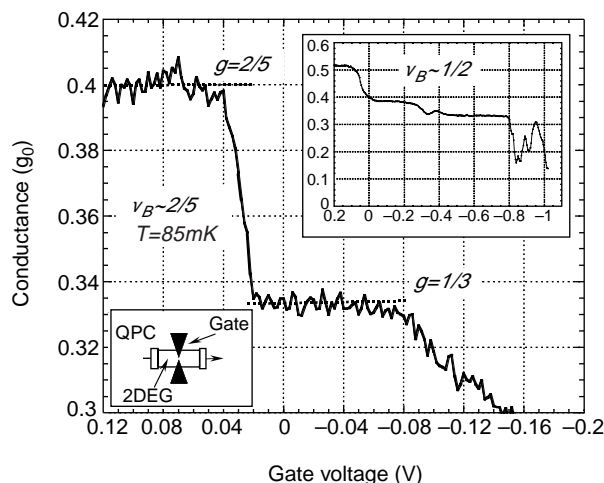


Figure 1 Two-terminal conductance (in units of the quantum conductance) versus voltage applied to the gates of the quantum point contact (QPC). Clear plateaux of $(2/5)g_0$ and $(1/3)g_0$ are seen for bulk filling factor $\nu_B = 2/5$ ($B = 12$ T). Top inset, a similar two-terminal conductance plot for a bulk filling factor of $\nu_B = 1/2$ ($B = 10.5$ T). Note that for zero voltage on the gates of the QPC the value of the conductance, in both cases, was lower than the bulk value ($g < \nu g_0$). This is a result of unintentional reflection from the QPC even when it is not biased. Indeed, when a small positive gate voltage was applied to the QPC the conductance increased and reached its bulk value. Application of a negative gate voltage recovered the $2/5$ and $1/3$ states, as expected. Bottom inset, schematic of the QPC in 2DEG. The QPC was formed by evaporating two metallic gates onto the surface of the heterostructure. By applying bias to the gates with respect to the 2DEG, the transmission of the incoming current through the small opening of the QPC is controlled. The electron temperature was determined by comparing the thermal noise without an external current through the QPC to the Johnson-Nyquist formula $S = 4k_B T g$ via $T = (\delta S / \delta g) / 4k_B$, with g the total conductance. Moreover, extrapolating this linear dependence to zero conductance (of the QPC) gives the contribution of our preamplifier to the total noise.

† Present addresses: Physics Department, Technion, Haifa 32000, Israel (M.R.); Bell Laboratories, Lucent Technologies, Murray Hill, New Jersey 07974, USA (R.d.P.).

smaller, channel-dependent, value δg_p . For example, the contribution of the first CF channel to the conductance is $\delta g_1 = g_0/3$ while that of the second channel is $\delta g_2 = (\frac{2}{5} - \frac{1}{3})g_0$. Hence, when the two lowest CF channels are fully transmitted the higher channel carries only a small portion (1/6) of the total current. Taking into account the smaller charge of the corresponding quasiparticle, $e/5$, a very weak shot-noise signal is expected. This makes the measurement of the noise in the 2/5 channel exceedingly difficult.

Our experiment was performed with a set-up similar to the one used in refs 4 and 17. Noise was measured within a bandwidth of ~ 30 kHz about a central frequency of 1.68 MHz. This frequency was chosen by tuning a LRC resonant circuit, with C the capacitance of the coaxial cables and R being mainly the resistance of the QPC. By choosing a two-fold lower frequency compared to the one used previously (4 MHz)⁴ we reduced the spurious noise contribution of our preamplifier from $1.1 \times 10^{-28} \text{ A}^2 \text{ Hz}^{-1}$ before to $3.8 \times 10^{-29} \text{ A}^2 \text{ Hz}^{-1}$. The preamplifier, which operates at 4.2 K, was manufactured from transistors fabricated with a GaAs-AlGaAs heterostructure grown in our own molecular beam epitaxy system. Measurements were performed in a dilution refrigerator at an electron temperature $T = 85 \text{ mK}$.

The 2DEG was embedded in a GaAs-AlGaAs heterostructure with a low-temperature carrier concentration $n_s = 1.15 \times 10^{11} \text{ cm}^{-2}$ and mobility $4.2 \times 10^6 \text{ cm}^2 \text{ V}^{-1} \text{ s}^{-1}$. A perpendicular magnetic field of $\sim 12 \text{ T}$ led to a bulk filling factor 2/5. The measured two-terminal conductance of two different runs, at bulk filling factors $\nu = 2/5$ and $\nu \approx 1/2$, as a function of applied voltage to the QPC gates, are shown in Fig. 1. Two clear conductance plateaux are seen near $g = (2/5)g_0$ and $g = (1/3)g_0$.

In the absence of an exact model for shot noise at $\nu = 2/5$, we compare our results with the partition noise expected from non-interacting particles. In other words, we assume that the scattering events of the quasiparticles at the QPC are independent. This assumption has been quite successful in analysing the noise results for quasiparticles with charge $e/3$ in a single CF channel^{4,5}. At zero temperature ($T = 0$), one would expect the low-frequency spectral density of current fluctuations, S , to be given by:

$$S_{T=0} = 2qV\delta g_p t_p (1 - t_p) \quad (1)$$

with V the applied bias voltage across the QPC, δg_p the contribution of the p th CF channel to the total conductance, t_p the transmission

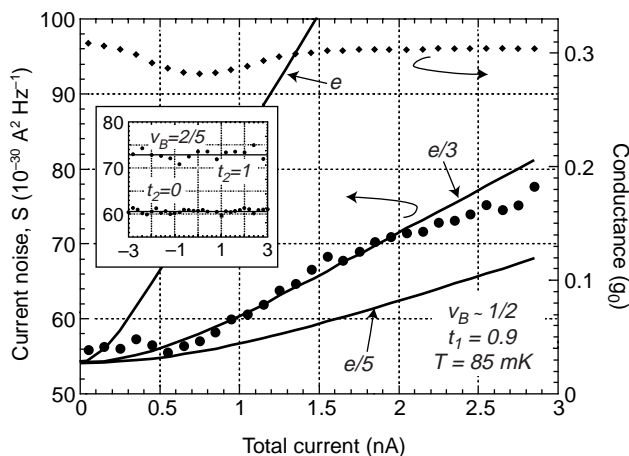


Figure 2 Measured spectral density of current fluctuations for $t_1 = 0.9, t_2 = 0$. The 2/5 channel is fully reflected (filled circles, left-hand vertical axis). The result agrees well with a quasiparticle charge $q = e/3$ and $T = 85 \text{ mK}$ substituted in equation (2) and is in excellent agreement with ref. 4. For comparison, the expected noise curves for quasiparticle charge $q = e/5$ and $q = e$ are shown. The inset shows the noise measured at both 2/5 ($t_1 = 1, t_2 = 1$) and 1/3 ($t_1 = 1, t_2 = 0$) plateaux. No excess noise is measured on the plateaux as no partitioning takes place and the reservoirs produce a noise-free current.

coefficient of this channel, and q the charge of the quasiparticle¹⁴. For example, for $p = 2$, $\delta g_2 = g - g_0/3$ and $t_2 = [(g/g_0) - 1/3]/(2/5 - 1/3)$.

A more subtle issue is the expected noise at a finite temperature T . This noise does not vanish at zero applied voltage but approaches the Johnson–Nyquist formula: $S = 4k_B Tg$, in accordance with the fluctuation-dissipation theorem. When a bias voltage V is applied, the noise is expected to increase smoothly with increasing V , approaching the linear behaviour predicted by equation (1) at an applied voltage greater than $V_T \approx 2k_B T/q$. Analytical expressions which take heuristically into account fractional statistics of the quasiparticles but ignore interactions among them¹⁸ lead to results that are very close to the one derived for non-interacting fermions with the electronic charge e replaced by the quasiparticle charge. On the other hand, numerical calculations¹⁹ that were done only for the

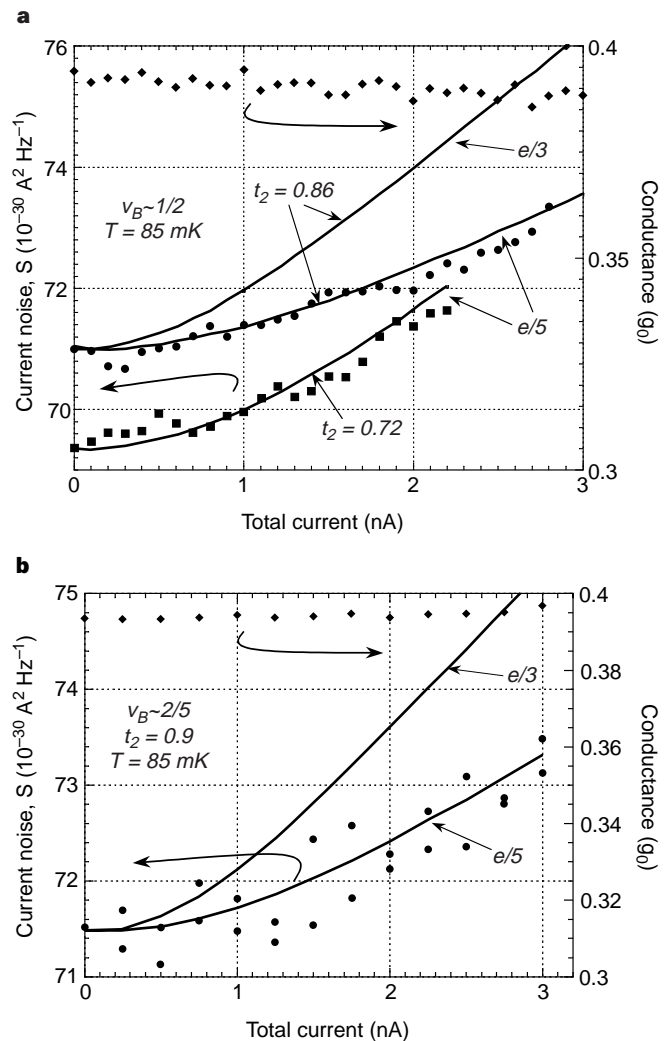


Figure 3 Measured noise of quasiparticles in the second composite fermion (CF) channel. The first CF channel (the '1/3' channel) is fully transmitted and does not produce noise (as seen Fig. 2 inset). **a**, Spectral density of current fluctuations against the total average current for transmission $t_2 = 0.86$ and $t_2 = 0.72$ at bulk filling factor $\nu_B = 1/2$ (filled circles, left-hand vertical axis). Solid lines are given by equation (2) assuming a charge $q = e/3$ and $q = e/5$ and $T = 85 \text{ mK}$ —as indicated. The sample's differential conductance, for transmission $t_2 = 0.86$ is also shown (filled diamonds, right-hand vertical axis). Note that the differential conductance, and hence the deduced transmission, are rather constant over the full range of the measurement. **b**, Similar noise and conductance data for $t_2 = 0.9$ and bulk filling factor $\nu_B = 2/5$. We note that there are no fitting parameters in the theoretical curves, as the transmission coefficient t_2 and the temperature of the electrons T are both measured independently^{4,17}.

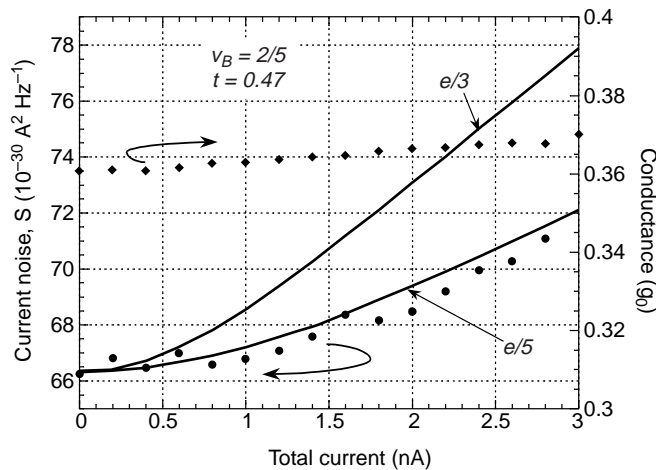


Figure 4 Current noise and conductance plotted against total average current. The measured spectral density of current fluctuations is given for relatively small transmission coefficient, $t_2 = 0.47$ (filled circles, left-hand vertical axis). Solid lines are given by equation (2) assuming charges of $q = e/3$ and $q = e/5$ —as indicated. The sample's differential conductance is also shown (filled diamonds, right-hand vertical axis). The transmission t_2 is determined by the average differential conductance over the full current range. We note, though, that the differential conductance in this case is not entirely independent of the applied voltage. In

general, a nonlinear I - V characteristic complicates the interpretation of our measurements: however, we expect the modifications to equation (2), due to the energy dependence of t_2 , are small. Apart from possible channel mixing, a change in the conductance by a relatively small amount induces a maximal change in the thermal noise $4k_B T \delta g$ of some 25% of the measured excess noise. Also, the weak dependence of the expected shot noise on t_2 near $t = 0.5$ (in a non-interacting-fermions picture) makes this nonlinearity insignificant.

fractional state $1/3$ contain parameters that are difficult to obtain experimentally. Hence we employ the expression for non-interacting particles²⁰ that was used successfully in the interpretation of the measurements in the $1/3$ fractional state⁴:

$$S = 2qV\delta g_p t_p (1 - t_p) \left[\text{ctanh} \left(\frac{qV}{2k_B T} \right) - \frac{2k_B T}{qV} \right] + 4k_B T g \quad (2)$$

We start with noise measurements on the conductance plateaux. The inset in Fig. 2 shows the results on both the $2/5$ ($t_2 = 1, t_1 = 1$) and $1/3$ ($t_2 = 0, t_1 = 1$) plateaux. We find no excess noise (above the thermal noise) within the accuracy of the measurement. This shows that the impinging current in both cases is noiseless, as one would expect for two independent CF channels. We come to this point later again. To tie the present results with previous experiments, we start with measurements of noise generated by partly reflecting the first CF channel (the $1/3$ channel). To validate our previous measurements of the charge $e/3$ and to verify that only the partitioning at the QPC is important in the determination of the charge, a different bulk filling factor, $\nu_B = 1/2$, was chosen (a bulk filling factor $1/3$ was employed before). Figure 2 shows the measured noise for a QPC partly reflecting the first CF channel and fully reflecting all the higher CF channels. The data, after calibration and subtraction of the amplifier's contribution, agree very well with the predicted shot noise with $q = e/3$.

The current noise for weakly back-scattered quasiparticles in the second CF channel, at two different bulk filling factors, is shown in Fig. 3. Figure 3a shows the measured noise for two values of the transmission of the QPC, $t_2 = 0.86$ and $t_2 = 0.72$, at a bulk filling factor $\nu_B \approx 1/2$. Using a quasiparticle charge $q = e/5$ and transmission deduced from the average value of the conductance (within the applied direct current range), the measured noise agrees well with the prediction of equation (2) throughout the whole range of direct current. Similarly, Fig. 3b shows the noise data for a different bulk filling, $\nu_B = 2/5$ and $t_2 = 0.9$. Even though the signal is weak and scattering of the data points is relatively large, it clearly verifies that the charge of the quasiparticles is $q = e/5$. Here, again, we see a clear manifestation of transport in the second CF channel with no contribution of the first CF channel (which is fully transmitted), as one would expect for non-interacting CF channels.

A similar agreement, even though surprising, between the measured noise and equation (2) is also obtained with a smaller transmission coefficient (within the range $0.4 < t_2 < 0.6$), as is demonstrated by the example in Fig. 4. Again a charge $q = e/5$ is measured. Theories^{6,7} find a smooth variation of the measured quasiparticle's charge from $q = e/3$ for weak back scattering to $q = e$ for strong back scattering, in the first CF channel ($\nu = 1/3 \rightarrow \nu = 0$ at the QPC). Extending such arguments to the transition $\nu = 2/5 \rightarrow \nu = 1/3$ within the QPC region, one would expect to determine via shot-noise measurements a charge $q = e/5$ at large t_2 changing monotonically to $q = e/3$ at small t_2 . Strong conductance variations with current for even stronger back reflection of the second CF channel ($t_2 < 0.4$) prevents accurate measurements of the shot noise and deduction of the value of the quasiparticle charge. □

Received 14 January; accepted 12 March 1999.

- Laughlin, R. B. Anomalous quantum Hall effect: an incompressible quantum fluid with fractional charge excitations. *Phys. Rev. Lett.* **50**, 1395–1398 (1983).
- Laughlin, R. B. Primitive and composite ground states in the fractional quantum Hall effect. *Surf. Sci.* **142**, 163–172 (1984).
- Prange, R. E. & Girvin, S. M. (eds) *The Quantum Hall Effect* (Springer, New York, 1987).
- de Picciotto, R. *et al.* Direct observation of a fractional charge. *Nature* **389**, 162–164 (1997).
- Saminadayar, L., Glatli, D. C., Jin, Y. & Etienne, B. Observation of the $e/3$ fractionally charged Laughlin quasiparticles. *Phys. Rev. Lett.* **79**, 2526–2529 (1997).
- Kane, C. L. & Fisher, M. P. A. Nonequilibrium noise and fractional charge in the quantum Hall effect. *Phys. Rev. Lett.* **72**, 724–727 (1994).
- Fendley, A., Ludwig, W. W. & Saleur, H. Exact nonequilibrium dc shot noise in Luttinger liquids and fractional quantum Hall devices. *Phys. Rev. Lett.* **75**, 2196–2199 (1995).
- de Chamon, C., Freed, D. E. & Wen, X. G. Tunneling and quantum shot noise in Luttinger liquids. *Phys. Rev. B* **51**, 2363–2378 (1995).
- Jain, J. K. Composite-fermion approach to the fractional quantum Hall effect. *Phys. Rev. Lett.* **63**, 199–202 (1989).
- Halperin, B. In *New Perspectives in Quantum Hall Effect* (eds Das Sarma, S. & Pinzuk, A.) 225–263 (Wiley, New York, 1997).
- Lesovik, G. B. Excess quantum shot noise in 2D ballistic point contacts. *JETP Lett.* **49**, 592–594 (1989).
- Reznikov, M., Heiblum, M., Shtrikman, H. & Mahalu, D. Temporal correlations of electrons: suppression of shot noise in a ballistic point contact. *Phys. Rev. Lett.* **75**, 3340–3334 (1995).
- Kumar, A., Saminadayar, L., Glatli, D. C., Jin, Y. & Etienne, B. Experimental test of the quantum shot noise reduction theory. *Phys. Rev. Lett.* **76**, 2778–2781 (1996).
- Reznikov, M. *et al.* Quantum shot noise. *Superlattices Microstruct.* **23**, 901–915 (1998).
- de Picciotto, R. Shot noise of non-interacting composite fermions. Preprint cond-mat/982221 at (xxx.lanl.gov) (1998).
- Sandler, N. P., de Chamon, C. & Fradkin, E. Noise measurements and fractional charge in fractional quantum Hall liquids. *Phys. Rev. B* (in the press); preprint cond-mat/9806335 at (xxx.lanl.gov) (1998).
- de Picciotto, R. *et al.* Direct observation of a fractional charge. *Phys. B* **249**–251, 395–400 (1998).
- Isakov, S., Martin, T. & Ouvry, S. Conductance and shot noise for particles with exclusion statistics. Preprint cond-mat/9811391 at (xxx.lanl.gov) (1998).

19. Fendley, P. & Saleur, H. Nonequilibrium dc noise in a Luttinger liquid with an impurity. *Phys. Rev. B* **54**, 10845–10854 (1996).
 20. Martin, Th & Landauer, R. Wave packet approach to noise in multichannel mesoscopic systems. *Phys. Rev. B* **45**, 1742–1755 (1992).

Acknowledgements. We thank G. Bunin for manufacturing the transistors for the cooled preamplifier, and D. Mahalu for performing the e-beam lithography. This work was partly supported by the Israeli Science Foundation, the German-Israeli Foundation and the Israeli Ministry of Science.

Correspondence and requests for materials should be addressed to M.H. (e-mail: heiblum@wis.weizmann.ac.il)

Two types of avalanche behaviour in granular media

Adrian Daerr & Stéphane Douady

Laboratoire de Physique Statistique de l'ENS, 24 rue Lhomond, 75231 Paris CEDEX 05, France

The nature of the transition between static and flowing regimes in granular media^{1,2} provides a key to understanding their dynamics. When a pile of sand starts flowing, avalanches occur on its inclined free surface. Previously, studies³ of avalanches in granular media have considered the time series of avalanches in rotating drums⁴, or in piles continuously fed with material. Here we investigate single avalanches created by perturbing a static layer of glass beads on a rough inclined plane. We observe two distinct types of avalanche, with evidence for different underlying physical mechanisms. Perturbing a thin layer results in an avalanche propagating downhill and also laterally owing to collisions between neighbouring grains, causing triangular tracks; perturbing a thick layer results in an avalanche front that also propagates upwards, grains located uphill progressively tumbling down because of loss of support. The perturbation threshold for triggering an avalanche is found to decrease to zero at a critical slope. Our results may improve understanding of naturally occurring avalanches on snow slopes⁵ where triangular tracks are also observed.

The experiments are done on an inclined plane covered with velvet cloth. This surface is chosen so that the glass beads (180–300 μm in diameter), our granular material, have a larger friction with it than between themselves. A thin layer of grains can thus remain static on the plane up to a larger angle than if it were on a grain pile. We set the plane to an angle φ (larger than the pile angle φ₀) and pour glass beads abundantly at the top. The moving beads leave behind a static layer of uniform thickness h(φ) (arrow leading to point a in Fig. 1; the geometry of the system is shown in Fig. 1 inset). This effect is explained by the variation of the friction of the successive grain layers with their distance to the surface of the inclined slope⁶: it is maximum for the bottom layer, and decreases continuously to the value for a thick pile. The top static layer is that which has a large enough friction coefficient on the underlying layers μ(h) to come to a stop. At inclination angle φ, the friction coefficient of this top static layer is then μ(h) = tanφ. The measurements h(φ) of Fig. 1 thus give the variation of the coefficient of friction with depth⁷. We obtain a simple exponential decay as in ref. 7:

$$\mu(h) = \mu(\infty) + \Delta\mu[\exp(-h/h_0)] \quad (1)$$

with h₀ of the order of 2d, where d = 240 μm is taken as the mean diameter of the grains, and Δμ = μ(0) – μ(∞) is the difference between the friction coefficient at the plane and that in the pile.

This remaining static layer is dynamically stable. If we add some beads onto this layer, they move downwards like a drop of liquid, leaving the layer unaffected. We can even jolt the experiment sharply: the whole layer starts to move but ‘freezes’ again very quickly.

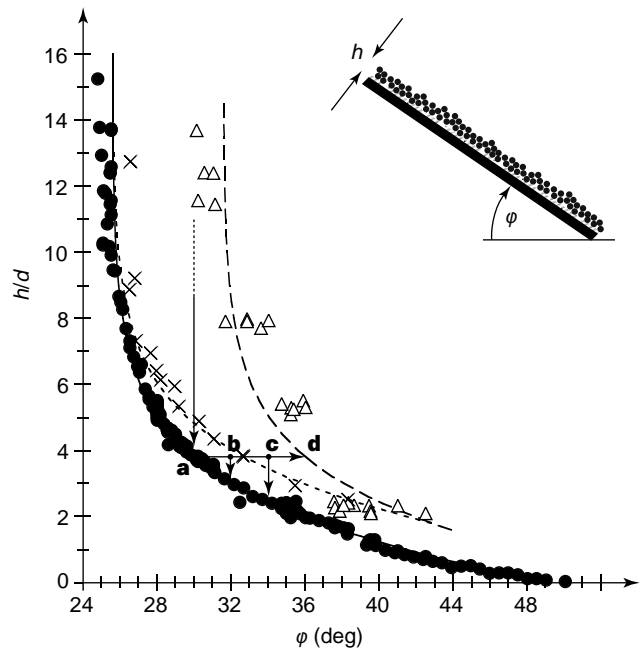


Figure 1 Stability diagram. Inset, the geometry of the experiment. Main figure, plot of h/d versus φ. The arrows sketch the course of an experiment. The filled circles show the measured thickness h of the layer left after a massive avalanche over the plane set at an angle φ (point a). The solid line is a fit according to equation (1). When these static layers are tilted they start flowing spontaneously at angles given by the open triangles (point d). The long-dashed line indicates the stability limit of a static layer. The hysteretic region between the solid and the long-dashed line is separated by the crosses (and the short-dashed line). Below them (for example, point b) a finite disturbance will generate a triangular avalanche. Above them (for example, point c) it will result in an avalanche front which also propagates uphill. For preparation angles φ > 34°, we observed only triangular avalanches (even the spontaneous ones). The precision of the measurements is smaller than the point size, and negligible compared to the physical fluctuations.

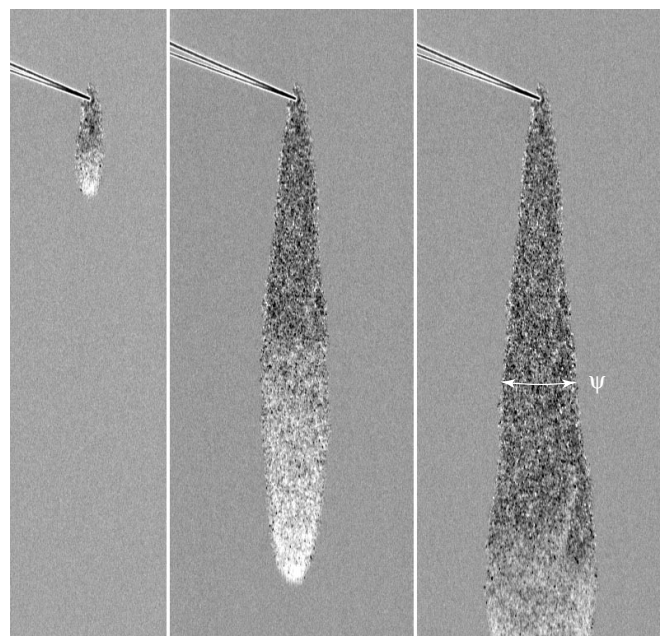


Figure 2 Evolution of a triangular avalanche (φ = 30°, δφ = 1.5°), showing the opening angle ψ. The time lapse between two images is 3.04 s. The pointed object is a pin used to trigger the avalanche, and indicates the origin of the avalanche.